A comparative proteomic analysis for non-invasive early prediction of hypoxic-ischemic injury in asphyxiated neonates

Sumrati Gurtoo
Yenepoya Research Centre, Yenepoya (Deemed to be University)
Gayathree Karthikkeyan
Yenepoya Research Centre, Yenepoya (Deemed to be University)
Santosh Kumar Behera
Yenepoya Research Centre, Yenepoya (Deemed to be University)
Chinmaya Narayana Kotimoole
Yenepoya Research Centre, Yenepoya (Deemed to be University)
Mohd. Altaf Najar
Yenepoya Research Centre, Yenepoya (Deemed to be University)
Prashant Kumar Modi
Yenepoya Research Centre, Yenepoya (Deemed to be University)
Sahana K.S.
Yenepoya Medical College and Hospital, Yenepoya (Deemed to be University)
Sneha M Pinto
Yenepoya Research Centre, Yenepoya (Deemed to be University)
Arun A.B. (quality@yenepoya.edu.in)
Yenepoya Institute of Arts Science Commerce and Management, Yenepoya (Deemed to be University

Research Article

Keywords: Comparative proteomics, Hypoxic-ischemic encephalopathy, Urinary biomarkers, Neurodevelopmental disorders, Diagnostic marker kit, Non-invasive biomarkers, Mass spectrometry

Posted Date: March 17th, 2023

DOI: https://doi.org/10.21203/rs.3.rs-2683506/v1

Additional Declarations: No competing interests reported.

Abstract

Aim:

Hypoxic Ischemic Encephalopathy (HIE) is one of the principal causes of neonatal mortality and long-term morbidity worldwide. The neonatal signs of mild cerebral injury are subtle, making an early precise diagnosis difficult. Delayed detection, poor prognosis, and lack of specific biomarkers for the disease are increasing mortality rates. In this study, we intended to identify specific biomarkers using comparative proteomic analysis to predict the severity of perinatal asphyxia so that its outcome can also be prevented.

Experimental Design:

A case-control study was conducted on 38 neonates, and urine samples were collected within 24

and 72 hours of life. A tandem mass spectrometry-based quantitative proteomics approach followed by validation via sandwich ELISA was performed.

Results:

The LC-MS/MS-based proteomics analysis resulted in the identification of 1,201 proteins in urine with 229, 244 and 426 being differentially expressed in HIE-1, HIE-2 and HIE-3, respectively. Axon guidance, Diseases of programmed cell death, and Detoxification of reactive oxygen species pathways were significantly enriched in mild HIE vs severe HIE. Of the differentially expressed proteins in various stages of HIE, we chose to validate four proteins- APP, AGT, FABP1, and FN1 via sandwich ELISA. Individual and cumulative ROC curves were plotted. AGT and FABP1 together showed high sensitivity, specificity, and accuracy as potential biomarkers for early diagnosis of HIE

Conclusion:

Establishing putative urinary biomarkers will facilitate clinicians to more accurately screen neonates for brain injury and monitor the disease progression. Prompt treatment of neonates may reduce mortality and neurodevelopmental impairment.

Statement Of Significance Of Study

Despite advances in monitoring technology and knowledge of fetal and perinatal medicine, the improvements in long-term neurological outcomes of neonates with hypoxic-ischemic encephalopathy (HIE) remain modest. The precise biomarkers for the early identification of neonates with subtle brain injury remain elusive. Using shotgun proteomics followed by ELISA, we validated a panel of four urinary proteins for predicting hypoxic injury in asphyxiated neonates within the first few hours of life. The cumulative ROC curve produced for AGT and FABP1 and APP and FN1 was significant for all the three stages of HIE. This makes it a highly sensitive prediction model with high accuracy, sensitivity, and specificity. After validation on a larger cohort, this combination of urinary biomarkers can be developed into a diagnostic kit for early identification of brain injury in asphyxiated neonates. It can also help in understanding the disease progression. The prompt treatment of neonates may also reduce mortality and neurodevelopmental impairment.

Background

Birth asphyxia or perinatal asphyxia is a clinical condition that arises due to the impaired gas exchange in neonates. It further leads to progressive hypoxia, hypercarbia, and acidosis, depending upon the extent and duration of the interruption. The interruption of oxygen supply causes energy failure and triggers a biochemical cascade, leading to cell dysfunction and death (1). The following criteria are considered for the diagnosis of asphyxia: (i) profound metabolic or mixed acidemia (pH < 7.00) in an umbilical artery blood sample, if obtained, (ii) persistence of an APGAR (Appearance, Pulse, Grimace, Activity, and Respiration) (score of 0–3 for longer than 5 min, (iii) neonatal neurologic sequelae (e.g., seizures, coma, hypotonia), and (iv) multiple organ involvement (e.g., kidney, lungs, liver, heart, intestines) (2). Globally 2.5 million newborn deaths occur annually, contributing to ~47% of the under-5 child mortality. Hypoxia of the newborn accounts for 30 to 35 percent and is the third most important cause of neonatal deaths, which is one million neonates every year worldwide (3). The frequency of perinatal asphyxia is approximately 3–5 in 1000 live births in developed countries with advanced obstetric and neonatal care. Each year, approximately a quarter of global neonatal deaths occur in India, with neonatal

mortality rate of 28 per 1000 live births and an infant mortality rate is 40–49 per 1000 live births (4, 5). Birth asphyxia can arise from several antepartum and intrapartum risk factors (6, 7). The severity and duration of the hypoxia are the most important factors determining the degree and the extent of organ and tissue damage associated with perinatal asphyxia. One of the outcomes of asphyxia is Hypoxic-ischemic encephalopathy (HIE). Due to a lack of oxygen and blood supply to the brain, the neurons are injured, and some even die. After assessing the severity of encephalopathy or insult by Sarnat and Sarnat staging criteria, HIE is categorized into three stages: HIE-1 (Mild), HIE-2 (Moderate), and HIE-3 (Severe). Hypoxia also has other adverse impacts such as respiratory distress syndrome, disseminated intravascular coagulation, subcutaneous fat necrosis, myocardial ischemia, adrenal hemorrhage, metabolic disorders, or acute tubular necrosis.

The current measures used to determine birth asphyxia include intrapartum electronic fetal monitoring, fetal or umbilical cord pH measurement, APGAR score, EEG, MRI, HIE, and major organ disorders (8). Early prediction of HIE is vital for selecting newborn infants who could benefit from neuroprotective treatment such as hypothermia (9) (10). Unfortunately, even when combining clinical signs and the current techniques, early identification of neonates, who may subsequently have a poor neurodevelopmental outcome, can still be challenging (11). This necessitates an urgent need to identify biomarkers that may aid in the early diagnosis of perinatal asphyxia and promptly identify neonates who require immediate attention for neuroprotection. Though the research in this field has been active in the last few decades, one of the biggest challenges lies with the prediction, detection, and grading of neonatal HIE, as this grading impacts the therapeutic intervention. The emergence of MS-based proteomic platforms as prominent bio-

analytical tools in clinical applications has enhanced the identification of protein-based urinary biomarkers (12, 13). Several studies have highlighted the specific role of a few promising biomarkers in the urine of the neonatal population, (14–17) however, none are routinely used in the clinic. Since urine sampling is minimally invasive compared to sampling of blood, urinary biomarkers are an important diagnostic approach.

For instance, the role of uromodulin (UMOD) and urinary neutrophil gelatinase-associated lipocalin (NGAL) in acute kidney injury (AKI) (18–20). Another biomarker that reflects the significant early steps in disease pathogenesis of necrotizing enterocolitis (NEC) is I-FABP(21–24) (AGT) is another biomarker extensively reported in the pediatric population to evaluate renal development and injury (25, 26)

In the present study, we employed a quantitative proteomics approach to identify urinary biomarkers to detect early brain injury in asphyxiated neonates with different stages of HIE- Mild (HIE-1), Moderate (HIE-2), and Severe (HIE-3). Our analysis revealed early biomarkers like Uromodulin (UMOD), Apolipoprotein-A2 (APOA2) for HIE-1 and also differential or severity biomarkers like Fatty Acid Binding Protein 1 (FABP1), Apolipoprotein-M (APOM), Parkinsonism Associated Deglycase (PARK7), Osteopontin (SPP1) for all the three HIE stages. The differentially expressed proteins were associated with neurodegenerative diseases, oxidative stress, amyloid fiber formation, and programmed cell death. This study may pave a path for identifying clinically relevant biomarkers specific to brain injury or its severity during birth asphyxia, which will further help to improve the therapeutic outcomes.

Methods

2.1 Study design

This case-control study was conducted in a tertiary care hospital in South India to identify candidate markers in the urine of neonates to predict birth asphyxia. The study included infants admitted and treated for birth asphyxia and its outcomes. The urine samples of both asphyxiated and healthy neonates were collected after obtaining approval from Institutional Ethical Committee (Study protocol no.YEC-1/2017/183). A written informed consent form was obtained from the parents of all the neonates. The asphyxiated and healthy (control) neonate's urine sample was collected in the pediatric uro bag (*Romsons)* and transferred to a sterile container. The first spot urine sample of the asphyxiated and healthy neonates was collected within 24 hours of life, and the second urine sample was taken only for asphyxiated neonates within 72 hours of life.

For the diagnosis of birth asphyxia, the following criteria were considered for the selection of neonates: APGAR score should be less than or equal to 5 at 5 minutes for birth asphyxia, evidence of encephalopathy using Sarnat and Sarnat staging, either evidence of fetal distress or assisted ventilation for at least 10 min after birth or evidence of any organ dysfunction, and ABG abnormality should be present at the time of birth for birth asphyxia. The samples with all birth weight categories and gestational age in neonates were included. The study excluded neonates with major congenital renal anomalies and maternal renal failure. (Supplementary File S1)

2.2 Clinical details

We collected the data on demographic details, risk factors for birth asphyxia, details of type of delivery with need for resuscitation and APGAR scoring. Postnatally the babies were assessed for the evidence of HIE using Sarnat and Sarnat staging and multiorgan dysfunction. Simultaneously need for ionotrophs and assisted ventilation were also recorded. Neonate's condition was monitored until discharge from NICU or death The biochemical parameters which are indicated in birth asphyxia were measured in blood as per institutional treatment protocol. These include Arterial blood gas (ABG), Renal function test (RFT), Serum electrolytes, and Septic screening parameters. The normal values of these parameters is given in Supplementary File S2. The identified biomarkers were correlated with the clinical severity of the disease.

2.3 Proteomics sample preparation for the discovery phase

The urine was centrifuged at 3000 rpm for 15 minutes at 4°C, and the supernatant of the urine was passed through a 0.22um PES filter. Then the urine was concentrated using an Amicon 3kDa filter unit (Amicon Ultra-15 Centrifugal Filter Unit, 15ml, Millipore, Catalog # UFC900396). The concentrated urine, the retentate, was transferred in cryovials and stored immediately at − 80°C. The estimated sample size for the discovery phase is 5 neonates in each condition (Healthy, HIE 1, HIE 2, and HIE 3). Protein concentration was estimated using the Bicinchoninic acid (BCA) assay, and the same was confirmed visually resolving on a 10% sodium dodecyl sulfate-polyacrylamide gel electrophoresis (SDS-PAGE) gel. Protein normalization was performed across all stages and all the four pooled conditions were split into two halves serving as technical replicates. Based on the protein concentrations, 250 µg of protein from each condition i.e 256µl, 416µl, 684.5µl and 737.6µl of concentrated urine from Healthy, HIE-1, HIE-2 and HIE-3

respectively was taken; protein cysteine bridges were reduced with 5mM dithiothreitol and alkylated with 10mM iodoacetamide. The proteins were then precipitated with 6x ice-cold acetone overnight at − 20°C. Precipitated proteins were reconstituted in 50 mM of TEABC and digested with TPCK-trypsin overnight at a ratio of 1:20 of enzyme/protein at 37°C. Digestion efficiency was evaluated by resolving the samples on 10% SDS-PAGE and by checking the percentage of peptides detected with 1 maximum missed cleaves. and it resulted in the identification of 15.99% and 17.33% of peptides with 1 missed cleaves. The peptides were dried overnight in SpeedVac and stored at − 20°C until labeling.

2.4 Tandem Mass Tag Labeling

Peptide samples were reconstituted in 50 mM of TEABC and were used for isobaric labeling with TMT 10plex kit (Thermo Fisher Scientific) as per the manufacturer's protocol. Peptides from the eight different samples were labeled with following TMT channels: i) Healthy 1- 126, and Healthy 2- 128C ii) HIE1,1- 127N, and HIE1,2- 131 iii) HIE2,1- 127C, and HIE2,2- 129C iv) HIE3,1- 128N, and HIE3,2- 129N. The respective TMT tags were added to all the samples, incubated at room temperature for 1 h, and quenched by adding 8µL of 5% hydroxylamine. The samples were pooled and dried overnight using SpeedVac. The dried samples were stored at − 20°C until fractionation.

2.5 Basic pH reverse-phase liquid chromatography (bRPLC)

The pooled sample consisting of labeled peptides was reconstituted using bRPLC solvent A (10 mM TEABC in water; pH 8.5) and loaded on the Xbridge C18 column (4.6 × 250 mm, 2.5 µm;

Waters, Milford, MA) and fractionated by basic pH reversed-phase liquid chromatography using a high-performance liquid chromatography (HPLC) system (Hitachi HPLC system-LC2400, Elite, LaChrom). In gradient mode, the peptides were separated by passing solvent B (10 mM TEABC in 90% acetonitrile, pH 8.5) at a 1 mL/min flow rate. The solvent B was increased from 3 to 50% over 120 mins. The peptides were fractionated into 96 fractions and concatenated to obtain six fractions. These fractions were dried and stored at − 20°C until LC-MS/MS analysis.

2.6 LC-MS/MS Analysis

All the six fractions were subjected to C18-based desalting, where each fraction was cleaned separately using C18 StageTip. The C18 bed was activated and equilibrated by passing 100% acetonitrile (ACN) and 0.1% formic acid (FA) at a slow rate. Peptides were reconstituted with 0.1% FA and loaded onto the C18 StageTip. Unbound contents were removed by a wash using 0.1% FA, and bound peptides were made to elute by passing elution buffer (0.1% FA in 40% ACN). The eluted peptides were dried and reconstituted in Mobile Phase A (0.1% FA) before the LC-MS/MS acquisition. Thermo Scientific Orbitrap Fusion Tribrid mass spectrometer (Thermo Fischer Scientific, Bremen, Germany) connected to Easy-nLC1200 nanoflow liquid chromatography system (Thermo Scientific) was used for data acquisition. Each fraction was reconstituted with Mobile Phase A and loaded onto a trap column (Acclaim PepMap™ 100, 75 µm X 2 cm,

nanoViper, C18, 3 µm, 100Å). Peptides bound to the trap column were separated and eluted by passing Mobile Phase B (0.1% FA in 80% ACN) through an analytical column (nanoViper, 75 µm silica capillary, 2 µm C18 Aq) at a flow rate of 300nl/min. The percentage of Mobile Phase B was increased gradually from 5% at 0 min to 40% in 75 min. This was further

increased to 70% in 23 mins, followed by 100% in another 7 mins, and kept at the same level for 15 mins. The total run time for each fraction was 120 mins. The analytical column temperature was set to 45°C throughout the sample acquisition process. The raw data was acquired in data-dependent acquisition (DDA) mode with a Top speed of 3 sec. The Orbitrap mass analyzer acquired peptide precursors within m/z of 400–1600 mass range at a mass resolution of 120K (200 m/z). Automatic gain control (AGC) target and maximum injection time (Max. IT) for precursor scan were set to $2e^5$ and 5 ms, respectively. Precursors with charge (z) state 2–8 and minimum intensity of $5e^4$ were isolated with a 1.6 m/z isolation window and fragmented in HCD with 34 ± 3%. The AGC target and Max.IT for the isolated precursors was set to $1e^5$ and 200 ms, respectively. The resulting fragments between 110–2000 m/z were acquired in Orbitrap mass analyzer at a mass resolution of 60K (200 m/z). The dynamic exclusion rate was set to the 30s. Data acquisition was carried out in technical triplicates for both the technical replicates.

2.7 Database Search for Peptide and Protein Identification

The raw data files were processed using Proteome Discoverer v2.2 (Thermo Fisher Scientific, Bremen, Germany). The data were searched against the human proteome (v109, RefSeq, NCBI) and common contaminant proteins databases using SequestHT and MASCOT search algorithms. The search was performed with trypsin and semi-trypsin as proteolytic enzymes separately. The remaining search parameters used were: a minimum peptide length of seven amino acids with one maximum missed cleavage. Precursor and fragment level mass tolerances were set at 10 ppm and 0.02 Da, respectively. Carbamidomethylation of cysteine (C) and TMT modification at the peptide N-terminus were set as fixed modifications. At the same time, TMT modification at the lysine

residues, oxidation of methionine (M), and acetylation of protein N-termini were set as dynamic modifications. False discovery rate (FDR) cut-off of 1% (q-value < 0.01) was applied at peptide spectrum match (PSM), peptide and protein level to remove false-positive identifications. Data normalization was carried out on the total peptide amount using Proteome Discoverer.

2.8 Validation by ELISA

We selected Amyloid-beta precursor protein (APP), fibronectin 1(FN1), fatty acid-binding protein (FABP1), and Angiotensinogen (AGT) from the significantly altered proteins identified in the discovery phase for validation. These biomarkers were monitored across different time points (24 hours and 72 hours) and were further validated in a larger cohort (n = 38) using sandwich ELISA (FN1, FABP1, APP from Wuhan Fine Biotech and AGT from Krishgen Biosystems). Due to the COVID-19 pandemic, we could collect n = 8 samples for HIE stage 3. The ELISA test was carried out as per the manufacturer's instructions and in duplicates. A semi-log regression model curve fit was applied to generate a standard curve. GraphPad Prism-5 was used for statistical analysis. One-way ANOVA with Tukey's post-hoc test was used to compare groups and different time points, and a p-value < 0.05 was considered significant. The candidate proteins were evaluated for their capacity to distinguish between healthy and asphyxiated neonates using receiver operating characteristic (ROC) curves based on the ELISA scores, which were calculated and plotted using an R script.

2.9 Data Analysis

The normalized protein abundances were imported into the Perseus software and analyzed for differential regulation and statistics. The abundance values were transformed to their log10 and tested for statistical significance with the ANOVA test with post-hoc Tukey's testing to determine the p-value and the significant pairs. The FDR corrected p-value (q-value) was also calculated using the Permutations-based FDR. The abundance values were used for the fold change calculations with respect to the healthy group, of which the proteins having an FC cut-off > 1.5 and < 0.67 were considered biologically significant. The Sankey diagram was generated using an online Sankey generator (http://sankey-diagram-generator.acquireprocure.com/). The differentially expressed proteins were categorized based on Gene Ontology analysis using David (Version 6.8), and pathway enrichment analysis was conducted using Enrichr (https://amp.pharm.mssm.edu/Enrichr/) and Reactome online tool (Version 71). The volcano plot (ggplot2 v3.4.0), correlation plot (corrplot v0.92, Hmisc v4.8), GoChord (GOplot v1.0.2), bubble plot (ggplot2 v3.4.0), heatmap (pheatmap 1.012), and ROC curves (pROC v1.18.0) were generated using the R program (v4.1.0). For interactome analysis, Cytoscape version 1.5 was used. One-way ANOVA was used to calculate the clinical parameter's p-value and 95% Confidence interval (CI). The Chi-square test and One-way ANOVA were performed to determine the p-value of the clinical parameters.

Results

3.1 Baseline characteristics of the asphyxiated neonates

A total of 10 healthy neonates and 28 asphyxiated neonates were recruited for this study. According to our study, females (35.7%) were less prone to birth asphyxia than males (64.3%), which was also statistically significant (p-value = 0.02). The term neonates (between 37–41 weeks) (82.1%) and normal-weight babies (2.5-3.5kg) (71.4%) were at higher risk of having birth asphyxia than preterm (< 37 weeks) (17.8%) and low (2.49-1.5kg) (17.9%) and very low (< 1.49kg) (10.7%) birth weight babies. The sample collection details, characteristics of the neonates, along with their antenatal

details, are presented in (Supplementary Table S1). Among the various risk factors associated with birth asphyxia, meconium-stained liquor was found statistically significant (p-value = 0.002). Low APGAR score can predict birth asphyxia. In our study, APGAR scoring at 1 min was below 3 for all the HIE-3 neonates and was statistically significant (p-value = < 0.001). Table 1 outlines the risk factors and neonatal characteristics of our study.

Table 1
Risk factors and neonatal characteristics in the study

Risk factors					
		HIE1 (n = 10)	**HIE2 (n = 10)**	**HIE3 (n = 08)**	**P-value**
Placenta praevia		0 (0%)	01 (10%)	0 (0%)	0.545
Records of NST monitoring		02 (20%)	03 (30%)	04 (50%)	0.040
Leaking PV		01 (10%)	0 (0%)	01 (10%)	0.385
Prolonged second stage		02 (20%)	03 (30%)	01 (12.5%)	0.111
Meconium stained liquor		04 (40%)	06 (60%)	06 (75%)	0.002
Neonatal data					
APGAR at 1 mins	Normal	0 (0%)	0 (0%)	0 (0%)	< 0.001
	Moderatelydepressed	06 (60%)	03 (30%)	0 (0%)	
	Severely depressed	04 (40%)	07 (70%)	08 (100%)	
APGAR at 5 mins	Normal	01 (10%)	0 (0%)	0 (0%)	< 0.001
	Moderately depressed	08 (80%)	10 (100%)	02 (25%)	
	Severely depressed	01 (10%)	0 (0%)	06 (75%)	
Required bag mask ventilation		10 (100%)	10 (100%)	08 (100%)	< 0.001
Required chest compressions		0 (0%)	01 (10%)	07 (87.5%)	0.057
Required drug (adrenaline)		01 (10%)	02 (20%)	05 (62.5%)	0.057
Required intubation		10 (100%)	10 (100%)	08 (80%)	< 0.001
HIE staging		10	10	08	NA

The details of biochemical parameters, including Arterial Blood Gas (ABG), Serum electrolytes used for the classification of birth asphyxia provided in Table 2. Most of the neonates in our study had metabolic acidosis, which is a common phenomenon in asphyxiated neonates. 19 (67%) neonates were having suspected sepsis, although only 4 had positive blood cultures. In our study, 14 (50%) and 10 (35%) had abnormal urea and potassium values with a significant p-value of 0.02 and 0.001, respectively. However, the levels of blood Creatinine, Calcium, and Sodium were not found to be significant for HIE staging. The Chi-square test and One-way ANOVA were performed to determine the p-value of these clinical parameters Hence in our study, there is a statistically significant correlation between few risk factors of birth asphyxia and clinical and biochemical parameters which are used to classify birth asphyxia.

Table 2
Clinical parameters of the study

		Mean ± Std. Dev	P-value	95% CI	
				Lower Bound	Upper Bound
GRBS (mg/dl)	HIE1	72 ± 17.6	0.062	59.4	84.6
	HIE2	65.8 ± 14.7		55.3	76.4
	HIE3	85.5 ± 18.4		70.1	100.9
	Total	73.6 ± 18.1		66.6	80.7
ABG pH	HIE1	7.3 ± 0.1	0.030	7.2	7.4
	HIE2	7.3 ± 0.1		7.2	7.4
	HIE3	7.2 ± 0.2		7.0	7.3
	Total	7.3 ± 0.2		7.2	7.4
ABG pCO2	HIE1	31.4 ± 8.9	0.550	25.0	37.8
	HIE2	36.4 ± 10.1		29.1	43.7
	HIE3	36.5 ± 15.7		23.4	49.6
	Total	34.6 ± 11.4		30.2	39.1
ABG pO2	HIE1	121.7 ± 44.5	0.432	89.8	153.5
	HIE2	130.3 ± 61.7		86.2	174.5
	HIE3	96.9 ± 57		49.3	144.6
	Total	117.7 ± 54.5		96.6	138.8
ABG HCO3	HIE1	17 ± 5.4	0.103	13.2	20.9
	HIE2	20 ± 8.3		14.1	25.9
	HIE3	13.2 ± 4.7		9.3	17.1
	Total	17 ± 6.8		14.4	19.6
RFT Urea	HIE1	27.5 ± 11.5	0.822	19.3	35.7
	HIE2	26.9 ± 17.4		14.4	39.4
	HIE3	23.4 ± 14.5		11.2	35.5
	Total	26.1 ± 14.3		20.6	31.6
RFT Creatinine	HIE1	6.7 ± 19.1	0.498	-6.9	20.4
	HIE2	0.9 ± 0.3		0.7	1.1
	HIE3	1.9 ± 2.7		-0.4	4.1
	Total	3.2 ± 11.4		-1.2	7.7
Sodium	HIE1	137.3 ± 3.8	0.454	134.6	140.0
	HIE2	137.4 ± 7		132.4	142.4
	HIE3	132.9 ± 13		122.0	143.8
	Total	136.1 ± 8.3		132.8	139.3
Potassium	HIE1	4.1 ± 0.4	0.061	3.9	4.4
	HIE2	5.3 ± 2.3		3.6	7.0
	HIE3	3.6 ± 0.7		3.0	4.2

	Total	4.4 ± 1.6		3.8	5.0
Chloride	HIE1	100 ± 2.9	0.953	97.9	102.1
	HIE2	100.6 ± 4.3		97.5	103.7
	HIE3	100.1 ± 6.2		94.9	105.3
	Total	100.3 ± 4.4		98.6	102.0
Calcium	HIE1	9.3 ± 0.8	0.584	8.7	9.9
	HIE2	9.3 ± 1.3		8.4	10.2
	HIE3	8.8 ± 1.4		7.6	10.0
	Total	9.2 ± 1.2		8.7	9.6

3.2 Quantitative proteomics highlights differentially altered proteins across different stages of HIE

We performed a global proteomic profiling of the urine samples of healthy and asphyxiated neonates categorized based on the severity of HIE (Stage 1-mild, Stage 2 moderate, and Stage 3-severe). For the discovery phase, 5 urine samples each were collected from neonates within 24 hours of their life for all the four groups. The schematic of the quantitative proteomic analysis followed by validation is provided in Fig. 1. In-depth comparative proteomic analysis identified

8,654 non-redundant peptides corresponding to 1,201 proteins, of which 1,095 were quantifiable. (Supplementary Figure S1A) (Supplementary File S3). The fold change (FC) of these 1201 proteins and their respective p-values and q-values are given in (Supplementary File S4).

A correlation matrix plot was generated to observe the pattern in which these four groups correlate with each other, which is shown in (Supplementary Figure S1B). The clustering of the groups is based on the biological replicates and technical triplicates. The Pearson's correlation coefficient was equal to 1, i.e., in the case of similar stages and their replicates. On the contrary, negative co-relation or minimal positive co-relation was observed when the three stages of HIE were related to healthy, indicating variance. The inter individual variability of proteins can help in differentially diagnosing between the different stages of HIE.

The fold change of protein expression was calculated with respect to the healthy neonate, i.e., control and different stages of HIE. Proteins with fold-change ratios of ≥ 1.5 and ≤ 0.66 were considered upregulated and downregulated respectively with biological relevance and p-value ≤ 0.05 as statistically significant (Supplementary File S5). Employing this cut-off, we identified significantly altered proteins in all HIE Stages. 229 (104-upregulated and 129-downregulated) proteins were differentially regulated in HIE-1 whereas 244 (105- upregulated and 139- downregulated) and 426 (173- upregulated and 253- downregulated) were found to be differentially regulated in HIE-2 and HIE-3 stages respectively. A total of 53, 36, and 209 proteins were exclusively found in HIE-1, HIE-2, and HIE-3 respectively. Some of these altered proteins for HIE-1 are UMOD, Lactotransferrin (LTF), Cellular Retinoic Acid Binding Protein 1 (CRABP1), Lymphocyte Cytosolic Protein 1 (LCP1). For HIE-2 are Ryanodine Receptor 1 (RYR1), Nucleoside Diphosphate Kinase 1 (NME1), Metallothionein 3 (MT3). And for HIE-3

Apolipoprotein A4 (APOA4), Peroxiredoxin 2 (PRDX2), Thrombospondin 4 (THBS4),

Alpha 2-HS Glycoprotein (AHSG) (Supplementary Figs. 1C, D, and E)

3.3 Functional Annotation Reveals Enrichment of Dysregulated Proteins

To better understand the functional relevance of the dysregulated proteins found in our study, GO enrichment analysis was performed. Analysis of the subcellular localization of proteins showed that intracellular organelle lumen (20.98%), collagen-containing extracellular matrix (17.84%) and secretory granule lumen (11.76%) were the most enriched terms. Similarly, extracellular matrix organization (9.6%), platelet degranulation (4.9%), and regulation of the apoptotic process (8.82%) were among the most enriched terms based on the biological process. Likewise, Proteins with endopeptidase inhibitor activity (4.5%), actin-binding (3.33%), and hormone activity (1%) were most enriched in molecular function category. The association between the top enriched GO terms and these differentially expressed proteins is illustrated by a chord plot in Fig. 2. (Supplementary File S6A, 6B, 6C).

Biological process classification revealed that the dysregulated proteins like APP, AGT, and S100A8 were involved in the positive regulation of response to external stimulus. Furthermore, the proteins like APP, B2M, and APOA1 were involved in amyloid fibril formation. The molecular functional analysis showed that proteins like APP, AGT, SERPINA10, SPOCK1, and FN1 were involved in endopeptidase inhibitor activity, actin-binding, growth factor activity, etc.

3.4 Clustering pattern and classification of differentially expressed proteins

K-means clustering analysis grouped the differentially expressed proteins into eight clusters Fig. 3A. To understand the significance of these dysregulated proteins in the context of HIE, pathway

enrichment analysis was carried out using the Enrichr and Reactome tool for each cluster (27). The significant pathways were identified ($p < 0.05$) and 3 clusters were selected for further analysis based on their relevance to the disease. The cluster 2, 3, and 5 were narrowed down for pathway enrichment analysis and some crucial pathways enriched in cluster 2 and 5 included disease of programmed cell death, neurodegenerative diseases, innate immune system, amyloid fiber formation and cluster 3 proteins were involved in pathways like integrin cell surface interactions, signal transduction, platelet degranulation. In addition to this, the metabolism of proteins and lipids was also enriched, illustrated in Fig. 3B. (Supplementary File 6D) provides the list of the enriched pathways and proteins involved in them.

As hypoxia and oxidative stress are two leading biochemical pathways that occur during birth asphyxia, we compared the altered proteins of our study against their known proteins. We observed that 32 and 40 altered proteins from our study were common in hypoxia and oxidative stress specific proteins (Supplementary Fig. 2A and 2B), respectively.

Interactome analysis of the differentially regulated proteins was carried out using Cytoscape Version 1.5 to identify the proteins which are interacting and found in different pathways like neurodegenerative diseases, innate immune system is secreted in urine. Nodes with different color gradients were used to visualize the network and identify the highly expressed proteins (based on fold change) in urine Fig. 3C. Some of the proteins with high expression in urine were Fibronectin 1 (FN1), Alpha-hemoglobin-stabilizing protein (AHSP), and Beta-2-microglobulin (B2M). This led us to understand which altered proteins involved in significant pathways were expressed in urine.

3.5 Classification of commonly altered proteins

To obtain more insights into the dysregulated proteins, a comparison between differentially expressed proteins of the different HIE stages was performed. Here, we observed 113 proteins commonly altered across all three conditions (Supplementary information Fig. 3A). Besides to that, we also found 53, 36 and 209 dysregulated proteins excusive to HIE1, HIE2, and HIE3 stages and these can potentially serve as stage-specific biomarkers. For instance, LTF, UMOD, and SPP1 specific to HIE1 can serve as early markers. A few examples along with their increasing expression trend across the three stages of HIE has been presented in Supplementary Table 2. A heat map was generated to explore the expression profile of these common and differentially expressed proteins (Supplementary Fig. 3B). Unsupervised clustering of the commonly altered proteins demonstrated global differences in protein expression patterns in the different stages of HIE compared to healthy. In contrast, technical replicates of each group clustered together. To deduce the various functions of these proteins, we carried out Gene Ontology (GO)-based classification using DAVID (Version 6.8). The most enriched biological process included platelet degranulation, extracellular matrix organization, neutrophil-mediated immunity, among others. Classification based on their subcellular localization revealed that the maximum number of proteins was localized to the intracellular organelle lumen, collagen-containing extracellular matrix, and secretory granule lumen. Similarly, the enriched terms in the molecular function were metal ion binding, calcium ion binding, cadherin binding, among others. (Supplementary Fig. 3C).

3,6 Validation of a selected panel of proteins by ELISA

Based on the expression pattern, biological and statistical significance, a panel of four proteins was selected for validation by sandwich ELISA. Of these four proteins, Angiotensinogen (AGT) and Fatty acid-binding protein (FABP1), were found to be significantly upregulated, and Amyloid-beta precursor protein (APP) and Fibronectin 1 (FN1), were found significantly downregulated. The FABP1 was upregulated across all the HIE stages within 24 hours while as AGT was upregulated in HIE-3. While the APP was downregulared in HIE-3 and FN1 for HIE-2 and HIE-3. (Supplementary Table 3). The expression of these four proteins was analyzed at two different time points, i.e., 24 hours for the healthy and asphyxiated neonates and 72 hours for the asphyxiated neonates. The expression of this panel of proteins was validated by sandwich-based ELISA using urine from 10 healthy neonates and 28 asphyxiated neonates (Supplementary File S7). Similar expression trend is observed between ELISA and mass spectrometry data (Table 3). All the four markers show a trend in their fold change in both the time points across the three stages of HIE. So, they might serve as differential biomarkers to distinguish between HIE stages. AGT and FABP1 were significantly upregulated in both the time points in the urine of neonates with HIE than the healthy neonates (Fig. 4A and C) and in agreement with our mass spectrometry findings (Fig. 4B and D).

Table 3
The differences in the mean concentration of early urine biomarkers in all the three stages of HIE in neonates from sandwich ELISA were compared with the mean concentration of healthy neonates and the same have been shown in fold change differences.

Protein	Healthy vs HIE_1_24	Healthy vs HIE_2_24	Healthy vs HIE_3_24	Healthy vs HIE_1_72	Healthy vs HIE_2_72	Healthy vs HIE_3_72
AGT	1.27	1.30	1.81	1.36	1.46	1.92
	***	***	***	***	***	***
FABP1	2.33	3.73	4.98	2.84	5.46	6.73
	***	***	***	***	***	***
APP	0.82	0.55	0.53	0.69	0.56	0.51
	***	***	***	***	***	***
FN1	0.63	0.43	0.32	0.40	0.42	0.30
	***	***	***	***	***	***
*** = p-value < 0.0001						

On the other hand, APP and FN1 were significantly downregulated in both the time points in the urine of neonates who were having HIE compared to the healthy neonates (Fig. 5A and C) and in agreement with our mass spectrometry findings (Fig. 5B and D). The maximum standard deviation for each protein in 24 hours was 21.8 for AGT, 22.45 for FABP1, 0.30 for APP, and 3.35 for FN1. The statistical summary of these four proteins is given in (Supplementary Table 4).

3.7 Receiver Operative Characteristic (ROC) analysis revealed a biomarker panel for early diagnosis of HIE

The ROC curve was plotted to observe the sensitivity and specificity of these four significantly dysregulated proteins, i.e., AGT (Fig. 6A), FABP1 (Fig. 6B), APP (Fig. 6C), and FN1 (Fig. 6D) in each stage of HIE. HIE cases and healthy control were selected as the dependent variable and protein levels as the independent variable. The ROC curves of these selected proteins were significant, with a p-value of < 0.0001 for all the stages of HIE. The summary of the ROC analysis is given in Table 4. The cumulative ROC curve was plotted for the upregulated proteins to comprehend their sensitivity, specificity, and accuracy as biomarkers. The ROC produced for AGT, and FABP1 was significant with a p-value < 0.0001 for all the three stages and area under the curve of 82.3%, 98.6%, and 100% for HIE stages 1, 2, and 3, respectively (Fig. 7A, C and E). A similar analysis was carried out for downregulated proteins APP and FN1, which revealed that the ROC curve for this model was also significant, with a p-value < 0.0001 for HIE stage 3, while the p-value for HIE stage 1 and HIE stage 2 was < 0.01 < 0.001, respectively. This model's area under the curve was 73.7%, 78.7%, and 84.6% % for HIE stages 1, 2, and 3, respectively (Fig. 7B, D, and F). The specificity of the model AGT and FABP1 was 95%, 95% and 100% and sensitivity was 58.9%, 97.3% and 100% for HIE stage 1, 2 and 3, respectively. On the other hand, for FN1 and APP the specificity was 100%, 100% and 80% along with the sensitivity of 46.1%, 55.8% and 76.9% for HIE stage 1, 2 and 3, respectively. Hence, the analysis revealed that AGT and FABP1 together formed a better model for all the stages of HIE. The characteristics of the ROC curve for these four proteins are exhibited in (Supplementary Table 5).

Table 4
Summary of Receiver Operative Characteristic (ROC) curve features for urine biomarkers

Protein	Condition	AUC (%)	95% CI (DeLong)	P-value	Threshold	Specificity	Sensitivity	Accuracy	Ppv	Npv	recall
FN1	HIE1	85.5	73.93–97.07	< 0.0001	5.874	75	85	80	77.3	83.3	85
	HIE2	100	100–100	< 0.0001	4.939	100	100	100	100.0	100.0	100
	HIE3	100	100–100	< 0.0001	4.481	100	100	100	100.0	100.0	100
APP	HIE1	96.75	92.4–100	< 0.0001	2.151	100	80	90	100.0	83.3	80
	HIE2	98.75	96.1–100	< 0.0001	1.913	95	100	97.5	95.2	100.0	100
	HIE3	100	100–100	< 0.0001	1.736	100	100	100	100.0	100.0	100
AGT	HIE1	93.25	84.85–100	< 0.0001	129.550	100	80	90	100.0	83.3	80
	HIE2	94.75	87.36–100	< 0.0001	132.900	95	85	90	94.4	86.4	85
	HIE3	100	100–100	< 0.0001	167.450	100	100	100	100.0	100.0	100
FABP1	HIE1	100	100–100	< 0.0001	73.660	100	100	100	100.0	100.0	100
	HIE2	100	100–100	< 0.0001	85.820	100	100	100	100.0	100.0	100
	HIE3	100	100–100	< 0.0001	113.320	100	100	100	100.0	100.0	100

Discussion

The extensive inception of therapeutic hypothermia as a standard of care for HIE has increased the pressure on clinicians to make an early and precise assessment of the degree of hypoxic injury (HI) that has occurred and the severity of the encephalopathy that will ensue (28). No single urine-based marker at present is robust enough to detect significant brain/hypoxic injury or predict its outcome. Combining clinical and biochemical data with 'omics' technology is currently the most likely path toward improved detection and prediction of outcomes in neonatal HIE (29–31).We performed this case-control cohort study intending to identify potential biomarker(s) for detecting early HI brain injury in asphyxiated neonates. We generated quantitative proteomics data to investigate diagnostic biomarkers of neonatal HIE. The differentially expressed urinary proteins between HIE neonates and healthy controls were screened at different time points. This led in identification of an early prognostic biomarker panel that may predict brain injury and disease progression in asphyxiated neonates, though further validation is required.

The clinical assessment of the asphyxiated neonates indicated that in our study, the predisposing factors like meconium stain liquor and male sex were statistically significant for developing birth asphyxia in concordance with previous literature (32, 33). The evaluation of renal function test (RFT), Arterial blood gas (ABG), and serum electrolytes are normal in healthy neonates. Their abnormality is one of the clinical indications of birth asphyxia. Previous literature shows the evidence of renal abnormalities and their correlation with the degree of asphyxia (34, 35). The degree of serum electrolytes, i.e., sodium, potassium, and calcium, is related to the severity of birth asphyxia (36, 37). This corresponds with our findings where urea and potassium were significant, with a p-value of 0.02 and 0.001, respectively. The abnormal ABG values revealed that most neonates were predisposed to metabolic acidosis (38). One of the outcomes of our study was probable sepsis which corresponds with the reported literature (39, 40).

The pathway analysis identified pathways like the disease of programmed cell death, neurodegenerative diseases (41), innate immune system (42), and amyloid fiber formation (43),has been associated with hypoxic injury and poor neurodevelopmental outcomes.

Similarly, enriched gene ontology terms like amyloid fibril formation, positive regulation of response to external stimulus, and hormone and growth factor activity might have a role in brain injury and poor neurodevelopmental outcomes.

Interestingly, we identified proteins in correlation with the disease pathways, and a panel of four proteins was shortlisted for validation. These four proteins were APP, FN1, FABP1, and AGT. We evaluated this panel of proteins as potential biomarkers for the early diagnosis of hypoxic injury. APP and FN1 were significantly downregulated, while AGT and FABP1 were upregulated in our data. As discussed below, the role of these proteins is well established in neonatal diseases but remains unexplored or markedly less in birth asphyxia and HIE.

FN1 is an extracellular matrix protein that plays a critical role in cytoskeletal organization, cell cycle progression, growth, and cell survival and differentiation (44). In our study, it is related to the pathways like post-translational protein modifications and degradation of the extracellular matrix. A study by Carlyle *et al.*,2017, an in-depth proteomic survey of postnatal human brain regions shows the expression of FN1 in amygdala, cerebellum, dorsolateral prefrontal cortex, hippocampus, medial dorsal nucleus of thalamus, primary visual cortex, and striatum regions of neonatal brain (45). FN1 is overexpressed in developing embryos and may also be involved in early blastocyst formation (46). The role of FN1 is not much explored in HIE, but the knowledge

of fetal FN results may reduce preterm birth before 37 weeks and its upregulation has been associated with preeclampsia (47, 48). Prematurity and preeclampsia are the risk factors for birth asphyxia (49). So, FN1 might have a role in birth asphyxia. In our study, it is showing a decreasing trend across all the stages of the HIE in 24-hour and 72-hour time points as observed by mass spectrometry and validated by ELISA.

AGT plays a crucial role in the pathophysiological modulation of cardiovascular functions. It is the primary trigger for generating reactive oxygen species (ROS) in various tissues (50). Public database such as BrainSpan Atlas of the Developing Human Brain shows AGT expression in 37 weeks after post conception and early postnatal (1-3years). The lack of AGT has also been associated with failure of BBB repair after an injury in mice (51). Also, the brain-specific renin-angiotensin system (RAS) plays essential role in brain homeostasis. One of the receptor i.e., AT_2R expression was found in developing fetal tissues, which reduces after birth and maintains a relatively low level during adulthood (52). Although there is less literature available showing the association of AGT with HIE (53), due to its role in BBB repair and brain homeostasis it might have a role to play in brain injury as well. Our validation experiment shows the increase in expression pattern at both time points with the severity of HIE.

APP is a transmembrane protein expressed mainly in the brain. It is responsible for neurodegenerative diseases like Alzheimer's (54) and has a significant role in the migration of nerve cells (55). APP accumulation in the brain is an early marker of brain injury, and the low plasma APP levels have been previously correlated with HIE progression (56, 57). An animal study conducted by Benterud *et al.* (2015) exhibited a similar drop in APP levels after neonatal

asphyxia (58). It was downregulated across all conditions at both time points and was associated with pathways like neurodegenerative disease and amyloid fiber formation. Hence, our findings for this protein resonates with the previous reported literature.

FABP1 is a cytoplasmic protein that participates in lipid metabolism (59). Elevated FABP disrupts the blood-brain barrier and causes cerebral ischemic injury in mice(60). Higher levels of FABP have been reported in the serum of neonates having a hypoxic injury (61). According to the Human Developmental Biology Resource (HDBR), the RNA-seq data of prenatal human brain development shows FABP1 expression in the cerebellum, medulla oblongata, and spinal cord regions of neonatal brain (62). Therefore, FABP1 is present in the brain of neonates and brain injury can release them to the circulatory system. However, a detailed study on this with negative controls (neonates with other diseases) can further substantiate this claim. In our study, the fold change of this upregulated protein increases with the severity of HIE, indicating the disease progression. The pathways associated with this protein in our study are cellular response to stress and innate immune system.

Birth asphyxia is a multifactorial disease; we compared and examined the collective effect of these proteins as opposed to their individual impacts. A multivariable biomarker panel approach is preferable as it offers accuracy, sensitivity, and specificity (63, 64). The cumulative ROC curve provides better prediction of the disease than individual ROC curve. Measuring a panel of proteins for efficient categorization of disease conditions from the healthy is more effective than measuring single proteins (65, 66). In our study, the ROC curve produced for AGT and FABP1 and APP and

FN1 was significant for all three stages of HIE. This makes it a highly sensitive prediction model with high accuracy, sensitivity, and specificity.

Our findings suggest the involvement and possible role of FN1, AGT, APP, and FABP1 in HIE, in a stage-dependent manner. These proteins can be developed as potential biomarkers for asphyxiated neonates with hypoxic injury. A rapid test detection kit when used in a hospital setting could aid in providing accurate disease diagnosis by complementing clinical examination and expertise of the clinician. It will also help to assess the treatment efficiency and prognosis of the disease. As this is a preliminary study, further studies are necessary to characterize and validate the functional role of these proteins in disease progression and brain injury.

Conclusion

Our quantitative study aimed to explore the urinary proteomic expression profile of the asphyxiated neonates using a high-throughput proteomics approach. We have developed an extensive catalog of differentially expressed proteins in HIE. The findings of this study enabled us to gain better insights into the disease pathology by relating the role of dysregulated proteins with their associated pathways. Our analysis and validation present a sensitive biomarker panel of four proteins that have the potential to be developed into a multiparameter rapid testing kit to explore its prospective in clinical settings. The biomarker panel developed in this study exhibits better diagnostic accuracy than the individual proteins. Also, as urine is non-invasive and easy to collect in neonates a urinary diagnostic kit has an additional advantage over other body fluid kits. The

development of a rapid detection kit can be helpful in the early screening of brain injury, which is a need for the hour.

Limitations

As this is a preliminary study, we have used a modest sample size (n = 38) for the validation of biomarker panel. Cross-validation of these potential biomarker panels in the clinical setting using a larger cohort is required to explore their potential as a biomarker for HIE detection. This will further confirm their accuracy, precision, sensitivity, specificity, and positive and negative predictive values for a probable biomarker. Another limitation is the absence of samples after the hypothermia treatment.

Abbreviations

AKI: Acute kidney injury, APGAR: Appearance, Pulse, Grimace, Activity, and Respiration, AUC: Area under the receiver operating characteristic curve, BBB: Blood-brain barrier, DEX: Differentially expressed, HIE: Hypoxic-ischemic encephalopathy, LC-MS/MS: Liquid chromatography with tandem mass spectrometry, ROC: Receiver operating characteristic curve, TMT: Tandem Mass Tag

Declarations

Ethics approval and consent to participate

This study was approved by Institutional Ethical Committee (Study protocol no.YEC-1/2017/183) and conducted in a tertiary care hospital in South India. The study included infants admitted and treated for birth asphyxia and its outcomes. The urine samples of both asphyxiated and healthy neonates were collected after a written informed consent from the parents of all the neonates.

Consent for publication

All authors consent to the publication of this manuscript.

Availability of data and materials

The MS raw data and the Proteome Discoverer-searched data have been publically made available by submitting to the ProteomeXchange Consortium (http://proteomecentral.proteomexchange.org)via the PRIDE repository with the data set identifier PXD031986 (Username: reviewer_pxd031986@ebi.ac.uk, Password: KWvdEmKe).

Competing interests

The authors declare no potential conflicts of interest with respect to the study.

Funding

This study was supported by a seed grant (YU/Seed grant/074-2018) provided by Yenepoya (Deemed to be University). Sumrati Gurtoo is a recipient of Senior Research Fellowship from the Indian Council of Medical Research (ICMR), Government of India.

Authors' contributions

Sahana K.S., and Sneha M Pinto conceptualized and designed the study, interpretation of the data, and reviewed and critically revised the manuscript.

Arun A.B conceptualized and designed the study, supervised the experiments, reviewed and critically revised the manuscript

Sumrati Gurtoo collected the samples and clinical data, carried out the lab experiments, analysis and interpretation of data, drafted and revised the manuscript.

Prashant Kumar Modi supervised the experiments and critically reviewed the manuscript for important intellectual content.

Mohd. Altaf Najar performed mass spectrometry data acquisition and initial data analysisSantosh Kumar Behera contributed substantially to data analysis

Gayathree Karthikkeyan, and Chinmaya Narayana Kotimoole contributed to analysis and interpretation of data and reviewed and revised the manuscript

All authors approved the final manuscript as submitted and agree to be accountable for all aspects of the work.

Acknowledgements

The authors thank Karnataka Biotechnology and Information Technology Services (KBITS), the Government of Karnataka, for the support to the Center for Systems Biology and Molecular Medicine at Yenepoya (Deemed to be University) underthe Biotechnology Skill Enhancement Programme in Multiomics Technology (BiSEP GO ITD 02 MDA 2017). The authors thank Yenepoya (Deemed to be University) for access to instrumentation.

References

1. Al-Macki N, Miller SP, Hall N, Shevell M. The spectrum of abnormal neurologic outcomes subsequent to term intrapartum asphyxia. Pediatr Neurol. 2009;41(6):399–405.
2. Morales P, Bustamante D, Espina-Marchant P, Neira-Pena T, Gutierrez-Hernandez MA, Allende-Castro C, et al. Pathophysiology of perinatal asphyxia: can we predict and improve individual outcomes? EPMA J. 2011;2(2):211–30.
3. Moshiro R, Mdoe P, Perlman JM. A Global View of Neonatal Asphyxia and Resuscitation. Front Pediatr. 2019;7:489.
4. Solevag AL, Schmolzer GM, Cheung PY. Novel interventions to reduce oxidative-stress related brain injury in neonatal asphyxia. Free Radic Biol Med. 2019;142:113–22.
5. Sankar MJ, Neogi SB, Sharma J, Chauhan M, Srivastava R, Prabhakar PK, et al. State of newborn health in India. J Perinatol. 2016;36(s3):3–S8.
6. Volpe JJ. Neurology of the newborn. Major Probl Clin Pediatr. 1981;22:1–648.
7. Rainaldi MA, Perlman JM. Pathophysiology of Birth Asphyxia. Clin Perinatol. 2016;43(3):409–22.
8. Herrera CA, Silver RM. Perinatal Asphyxia from the Obstetric Standpoint: Diagnosis and Interventions. Clin Perinatol. 2016;43(3):423–38.
9. Hankins GD, Koen S, Gei AF, Lopez SM, Van Hook JW, Anderson GD. Neonatal organ system injury in acute birth asphyxia sufficient to result in neonatal encephalopathy. Obstet Gynecol. 2002;99(5 Pt 1):688–91.
10. Michniewicz B, Szpecht D, Sowinska A, Sibiak R, Szymankiewicz M, Gadzinowski J. Biomarkers in newborns with hypoxic-ischemic encephalopathy treated with therapeutic hypothermia. Childs Nerv Syst. 2020;36(12):2981–8.
11. Martin RJ, Fanaroff AA, Walsh MC. Fanaroff and Martin's neonatal-perinatal medicine: diseases of the fetus and infant. 9th ed. Philadelphia: Saunders/Elsevier; 2011.
12. Beasley-Green A. Urine Proteomics in the Era of Mass Spectrometry. Int Neurourol J. 2016;20(Suppl 2):70–5.

13. Marimuthu A, O'Meally RN, Chaerkady R, Subbannayya Y, Nanjappa V, Kumar P, et al. A comprehensive map of the human urinary proteome. J Proteome Res. 2011;10(6):2734–43.
14. Cao XY, Zhang HR, Zhang W, Chen B. [Diagnostic values of urinary netrin-1 and kidney injury molecule-1 for acute kidney injury induced by neonatal asphyxia]. Zhongguo Dang Dai Er Ke Za Zhi. 2016;18(1):24–8.
15. Essajee F, Were F, Admani B. Urine neutrophil gelatinase-associated lipocalin in asphyxiated neonates: a prospective cohort study. Pediatr Nephrol. 2015;30(7):1189–96.
16. Saran A, Devegowda D, Doreswamy SM. Urinary Intestinal Fatty Acid Binding Protein for Diagnosis of Necrotizing Enterocolitis. Indian Pediatr. 2020;57(9):798–800.
17. Nair J, Kumar VHS. Current and Emerging Therapies in the Management of Hypoxic Ischemic Encephalopathy in Neonates.Children (Basel). 2018;5(7).
18. You R, Zheng H, Xu L, Ma T, Chen G, Xia P, et al. Decreased urinary uromodulin is potentially associated with acute kidney injury: a systematic review and meta-analysis. J Intensive Care. 2021;9(1):70.
19. Zhang Y, Zhang B, Wang D, Shi W, Zheng A. Evaluation of Novel Biomarkers for Early Diagnosis of Acute Kidney Injury in Asphyxiated Full-Term Newborns: A Case-Control Study. Med Princ Pract. 2020;29(3):285–91.
20. Naunova-Timovska S, Cekovska S, Sahpazova E, Tasic V. Neutrophil Gelatinase-Associated Lipocalin as an Early Biomarker of Acute Kidney Injury in Newborns. Acta Clin Croat. 2020;59(1):55–62.
21. Coufal S, Kokesova A, Tlaskalova-Hogenova H, Frybova B, Snajdauf J, Rygl M, et al. Urinary I-FABP, L-FABP, TFF-3, and SAA Can Diagnose and Predict the Disease Course in Necrotizing Enterocolitis at the Early Stage of Disease. J Immunol Res. 2020;2020:3074313.
22. Shaaban AIE, Alfqy OAE, Shaaban HMK, YH AM, Assar EH. Potential Role of Serum Intestinal Fatty Acid-Binding Protein as a Marker for Early Prediction and Diagnosis of Necrotizing Enterocolitis in Preterm Neonates. J Indian Assoc Pediatr Surg. 2021;26(6):393–400.
23. Coufal S, Kokesova A, Tlaskalova-Hogenova H, Snajdauf J, Rygl M, Kverka M. Urinary Intestinal Fatty Acid-Binding Protein Can Distinguish Necrotizing Enterocolitis from Sepsis in Early Stage of the Disease. J Immunol Res. 2016;2016:5727312.
24. Evennett NJ, Hall NJ, Pierro A, Eaton S. Urinary intestinal fatty acid-binding protein concentration predicts extent of disease in necrotizing enterocolitis. J Pediatr Surg. 2010;45(4):735–40.
25. Mayumi R, Murano Y, Yokota R, Nakao A, Miyazaki N, Hara T, et al. Urinary angiotensinogen in pediatric urinary tract infection. Pediatr Int. 2019;61(7):712–4.
26. Shono M, Urushihara M, Suga K, Watanabe N, Saijo T, Nakagawa R, et al. Enhanced angiotensinogen expression in neonates during kidney development. Clin Exp Nephrol. 2019;23(4):537–43.
27. Kuleshov MV, Jones MR, Rouillard AD, Fernandez NF, Duan Q, Wang Z, et al. Enrichr: a comprehensive gene set enrichment analysis web server 2016 update. Nucleic Acids Res. 2016;44(W1):W90–7.
28. Murray DM. Biomarkers in neonatal hypoxic-ischemic encephalopathy-Review of the literature to date and future directions for research. Handb Clin Neurol. 2019;162:281–93.
29. Zhu Y, Yun Y, Jin M, Li G, Li H, Miao P, et al. Identification of novel biomarkers for neonatal hypoxic-ischemic encephalopathy using iTRAQ. Ital J Pediatr. 2020;46(1):67.
30. Hou X, Yuan Z, Wang X, Cheng R, Zhou X, Qiu J. Peptidome analysis of cerebrospinal fluid in neonates with hypoxic-ischemic brain damage. Mol Brain. 2020;13(1):133.
31. Fruscalzo A, Londero AP, Orsaria M, Marzinotto S, Driul L, Di Loreto C, et al. Placental fibronectin staining is unaffected in pregnancies complicated by late-onset intrauterine growth restriction and small for gestational age fetuses. Int J Gynaecol Obstet. 2020;148(2):253–60.
32. Mohamed MA, Aly H. Impact of race on male predisposition to birth asphyxia. J Perinatol. 2014;34(6):449–52.
33. Aslam HM, Saleem S, Afzal R, Iqbal U, Saleem SM, Shaikh MW, et al. Risk factors of birth asphyxia. Ital J Pediatr. 2014;40:94.
34. Gupta BD, Sharma P, Bagla J, Parakh M, Soni JP. Renal failure in asphyxiated neonates. Indian Pediatr. 2005;42(9):928–34.
35. Zhang Y, Zeng HH. Renal Function Profiles in Preterm Neonates With Birth Asphyxia Within the First 24 H of Life. Front Pediatr. 2020;8:583540.
36. Thakur J, Bhatta NK, Singh RR, Poudel P, Lamsal M, Shakya A. Prevalence of electrolyte disturbances in perinatal asphyxia: a prospective study. Ital J Pediatr. 2018;44(1):56.

37. Basu P, Som S, Das H, Choudhuri N. Electrolyte status in birth asphyxia. Indian J Pediatr. 2010;77(3):259–62.
38. Shah PS, Raju NV, Beyene J, Perlman M. Recovery of metabolic acidosis in term infants with postasphyxial hypoxic-ischemic encephalopathy. Acta Paediatr. 2003;92(8):941–7.
39. Shah PS, Beyene J, To T, Ohlsson A, Perlman M. Postasphyxial hypoxic-ischemic encephalopathy in neonates: outcome prediction rule within 4 hours of birth. Arch Pediatr Adolesc Med. 2006;160(7):729–36.
40. Hakobyan M, Dijkman KP, Laroche S, Naulaers G, Rijken M, Steiner K, et al. Outcome of Infants with Therapeutic Hypothermia after Perinatal Asphyxia and Early-Onset Sepsis. Neonatology. 2019;115(2):127–33.
41. Tarkowska A. Hypoxic-Ischemic Brain Injury after Perinatal Asphyxia as a Possible Factor in the Pathology of Alzheimer's Disease. In: Pluta R, editor. Cerebral Ischemia. Brisbane (AU)2021.
42. Li B, Concepcion K, Meng X, Zhang L. Brain-immune interactions in perinatal hypoxic-ischemic brain injury. Prog Neurobiol. 2017;159:50–68.
43. Nalivaeva NN, Turner AJ, Zhuravin IA. Role of Prenatal Hypoxia in Brain Development, Cognitive Functions, and Neurodegeneration. Front Neurosci. 2018;12:825.
44. Polin RA. Role of fibronectin in diseases of newborn infants and children. Rev Infect Dis. 1990;12(Suppl 4):428–38.
45. Carlyle BC, Kitchen RR, Kanyo JE, Voss EZ, Pletikos M, Sousa AMM, et al. A multiregional proteomic survey of the postnatal human brain. Nat Neurosci. 2017;20(12):1787–95.
46. Goossens K, Van Soom A, Van Zeveren A, Favoreel H, Peelman LJ. Quantification of fibronectin 1 (FN1) splice variants, including two novel ones, and analysis of integrins as candidate FN1 receptors in bovine preimplantation embryos. BMC Dev Biol. 2009;9:1.
47. Berghella V, Saccone G. Fetal fibronectin testing for reducing the risk of preterm birth. Cochrane Database Syst Rev. 2019;7:CD006843.
48. Zhao M, Li L, Yang X, Cui J, Li H. FN1, FOS, and ITGA5 induce preeclampsia: Abnormal expression and methylation. Hypertens Pregnancy. 2017;36(4):302–9.
49. Nayeri F, Shariat M, Dalili H, Bani Adam L, Zareh Mehrjerdi F, Shakeri A. Perinatal risk factors for neonatal asphyxia in Vali-e-Asr hospital, Tehran-Iran. Iran J Reprod Med. 2012;10(2):137–40.
50. Wen H, Gwathmey JK, Xie LH. Oxidative stress-mediated effects of angiotensin II in the cardiovascular system. World J Hypertens. 2012;2(4):34–44.
51. Heithoff BP, George KK, Phares AN, Zuidhoek IA, Munoz-Ballester C, Robel S. Astrocytes are necessary for blood-brain barrier maintenance in the adult mouse brain. Glia. 2021;69(2):436–72.
52. Carey RM, Siragy HM. Newly recognized components of the renin-angiotensin system: potential roles in cardiovascular and renal regulation. Endocr Rev. 2003;24(3):261–71.
53. Chen HM, Gao LX, Wang JJ, Gao C. The correlation between AGT gene polymorphism and neonatal hypoxic-ischemic encephalopathy (HIE). Eur Rev Med Pharmacol Sci. 2019;23(5):2194–9.
54. Salminen A, Kauppinen A, Kaarniranta K. Hypoxia/ischemia activate processing of Amyloid Precursor Protein: impact of vascular dysfunction in the pathogenesis of Alzheimer's disease. J Neurochem. 2017;140(4):536–49.
55. Plummer S, Van den Heuvel C, Thornton E, Corrigan F, Cappai R. The Neuroprotective Properties of the Amyloid Precursor Protein Following Traumatic Brain Injury. Aging Dis. 2016;7(2):163–79.
56. Matschke J, Buttner A, Bergmann M, Hagel C, Puschel K, Glatzel M. Encephalopathy and death in infants with abusive head trauma is due to hypoxic-ischemic injury following local brain trauma to vital brainstem centers. Int J Legal Med. 2015;129(1):105–14.
57. Benavente-Fernandez I, Ramos-Rodriguez JJ, Infante-Garcia C, Jimenez-Gomez G, Lechuga-Sancho A, Lubian-Lopez S, et al. Altered plasma-type gelsolin and amyloid-beta in neonates with hypoxic-ischaemic encephalopathy under therapeutic hypothermia. J Cereb Blood Flow Metab. 2019;39(7):1349–54.
58. Benterud T, Pankratov L, Solberg R, Bolstad N, Skinningsrud A, Baumbusch L, et al. Perinatal Asphyxia May Influence the Level of Beta-Amyloid (1–42) in Cerebrospinal Fluid: An Experimental Study on Newborn Pigs. PLoS ONE. 2015;10(10):e0140966.
59. Loor JJ, Wang Y, Tang K, Zhang W, Guo W, Wang Y, et al. Fatty acid-binding protein 1 increases steer fat deposition by facilitating the synthesis and secretion of triacylglycerol in liver. PLoS ONE. 2019;14(4):e0214144.
60. Liao B, Geng L, Zhang F, Shu L, Wei L, Yeung PKK, et al. Adipocyte fatty acid-binding protein exacerbates cerebral ischaemia injury by disrupting the blood-brain barrier. Eur Heart J. 2020;41(33):3169–80.

61. Li M, Jiang L, Zhang H, Wang D, Zhang M, Zhang L. Clinical significance of elevated serum A-FABP and free fatty acid in neonates with hypoxic ischemic brain damage. Exp Ther Med. 2016;12(2):746–52.
62. Lindsay SJ, Xu Y, Lisgo SN, Harkin LF, Copp AJ, Gerrelli D, et al. HDBR Expression: A Unique Resource for Global and Individual Gene Expression Studies during Early Human Brain Development. Front Neuroanat. 2016;10:86.
63. Jain A, Kotimoole CN, Ghoshal S, Bakshi J, Chatterjee A, Prasad TSK, et al. Identification of potential salivary biomarker panels for oral squamous cell carcinoma. Sci Rep. 2021;11(1):3365.
64. Vargason T, Grivas G, Hollowood-Jones KL, Hahn J. Towards a Multivariate Biomarker-Based Diagnosis of Autism Spectrum Disorder: Review and Discussion of Recent Advancements. Semin Pediatr Neurol. 2020;34:100803.
65. Moi SH, Lee YC, Chuang LY, Yuan SF, Ou-Yang F, Hou MF, et al. Cumulative receiver operating characteristics for analyzing interaction between tissue visfatin and clinicopathologic factors in breast cancer progression. Cancer Cell Int. 2018;18:19.
66. deCastro BR. Cumulative ROC curves for discriminating three or more ordinal outcomes with cutpoints on a shared continuous measurement scale. PLoS ONE. 2019;14(8):e0221433.

Figures

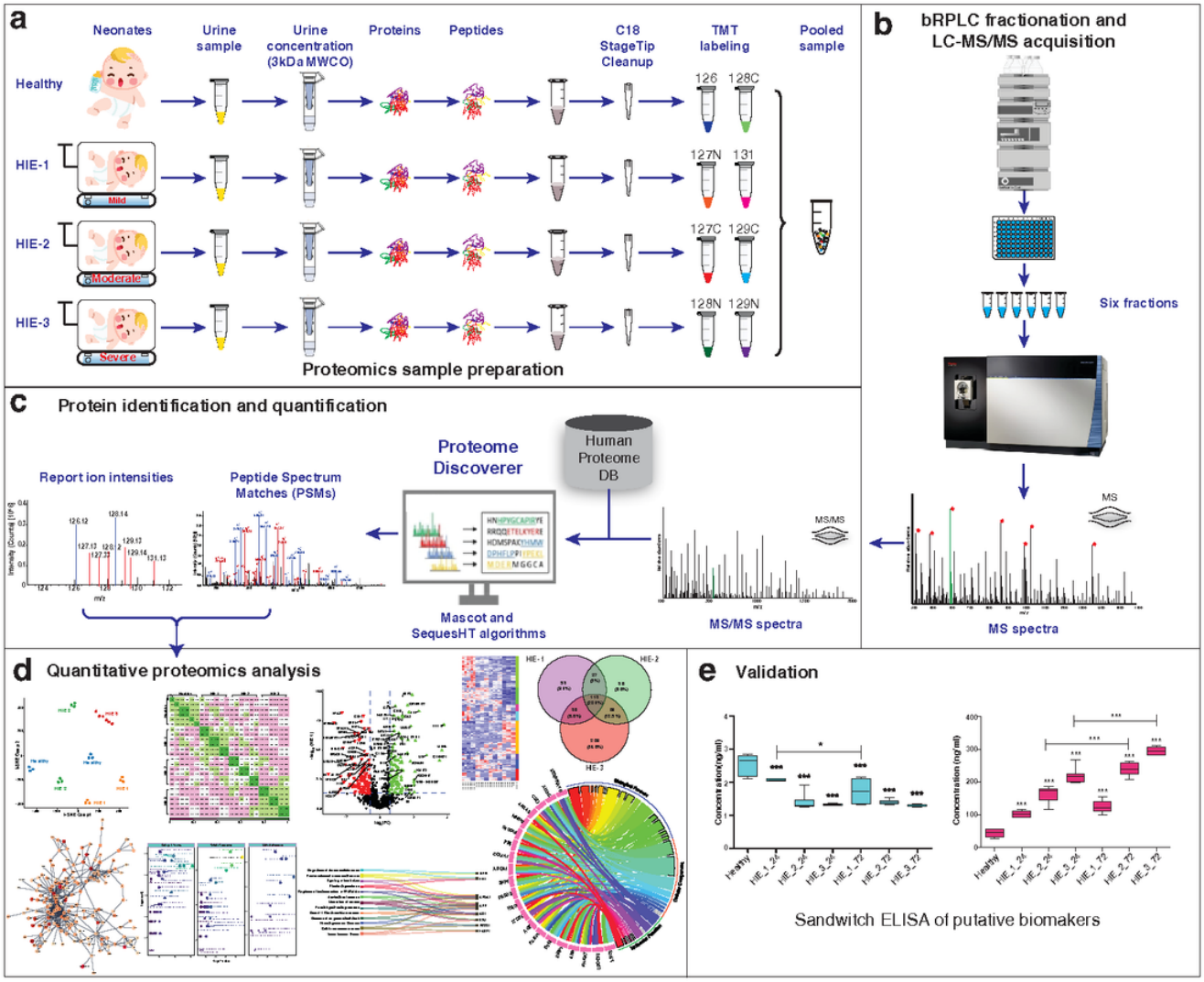

Figure 1

Graphical summary of the comparative urinary proteomics analysis by shotgun proteomics followed by validation using ELISA of healthy and asphyxiated neonates

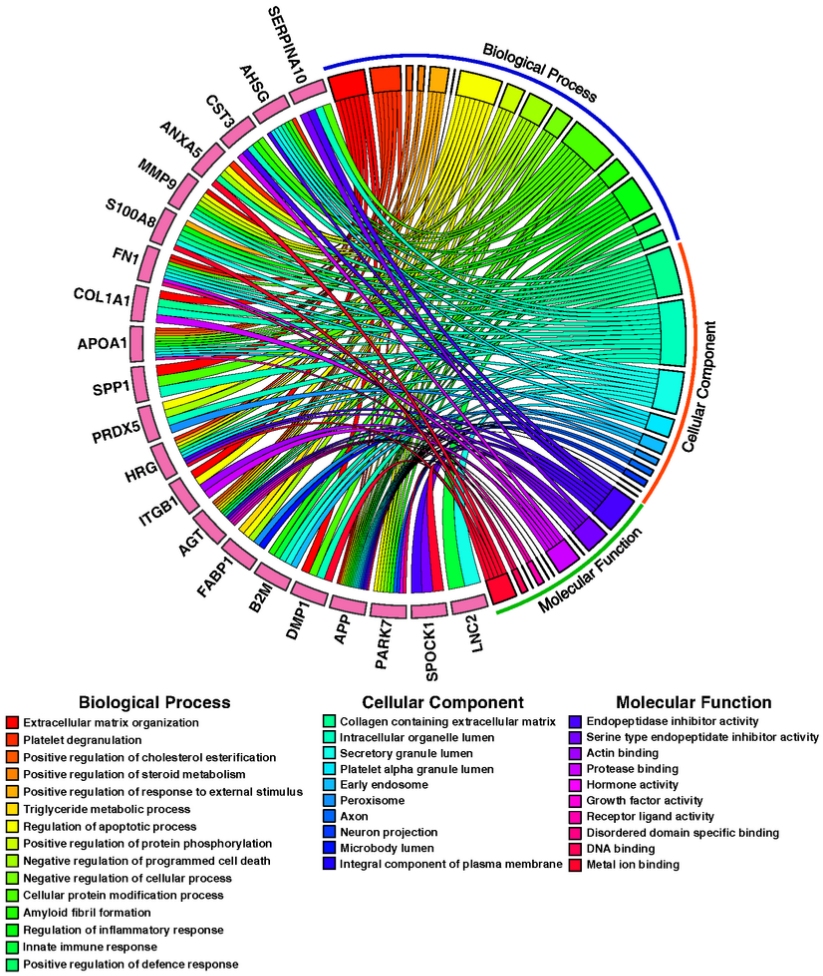

Figure 2

GO analysis of the differentially expressed (DEX) proteins. Gene ontology (GO) enrichment analysis of the biological process, cellular component, and molecular function of the DEX proteins. The chord plot displays the relationship between a few DEX proteins and the top enriched GO terms

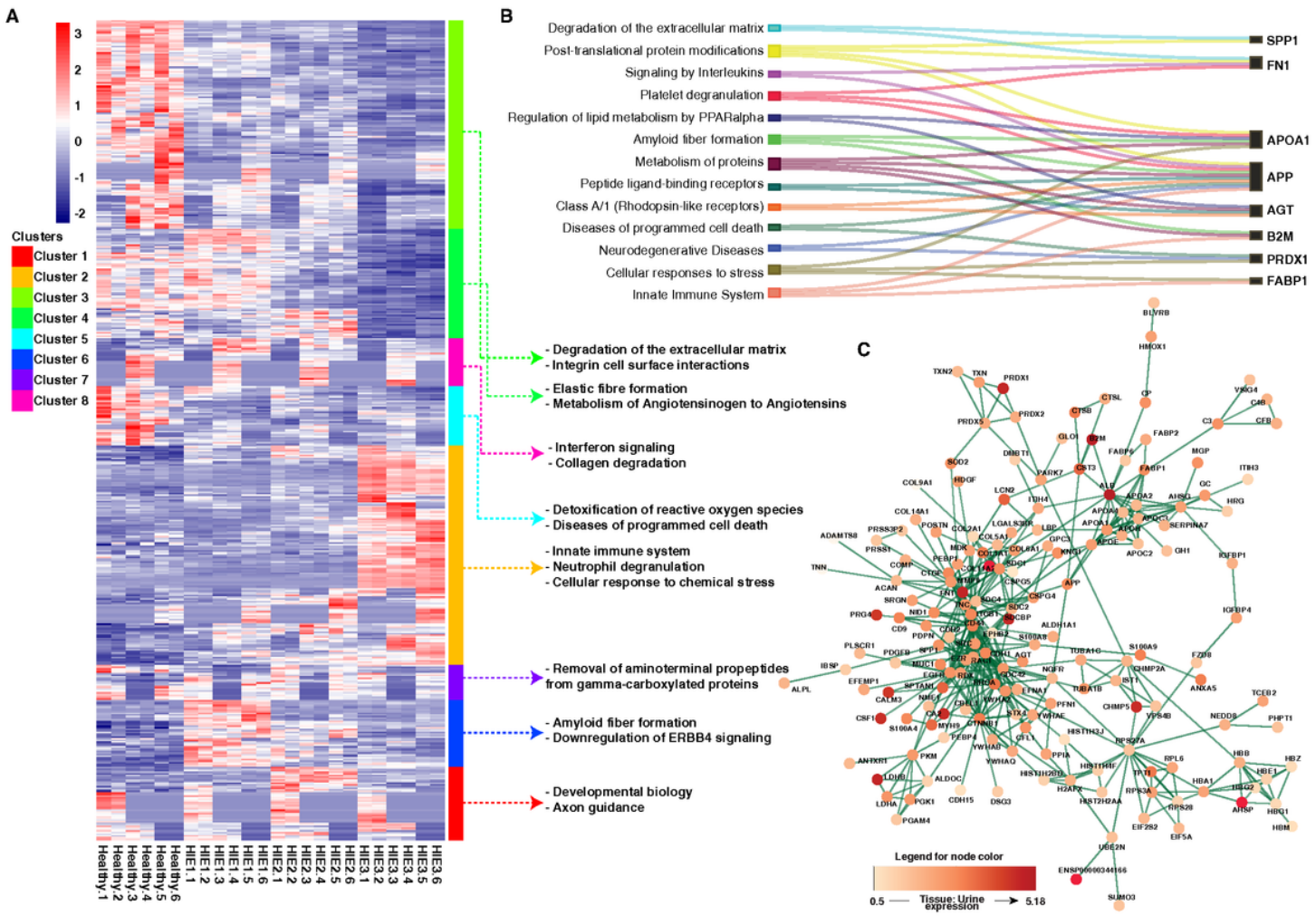

Figure 3

Clustering pattern of differentially expressed proteins. (A) Heatmap showing the hierarchical clustering of DEX urinary proteins in various stages of HIE. (B) Sankey diagram showing the involvement of DEX proteins in variousbiological pathways (C) Interactome analysis depictin expression of DEX proteins in urine

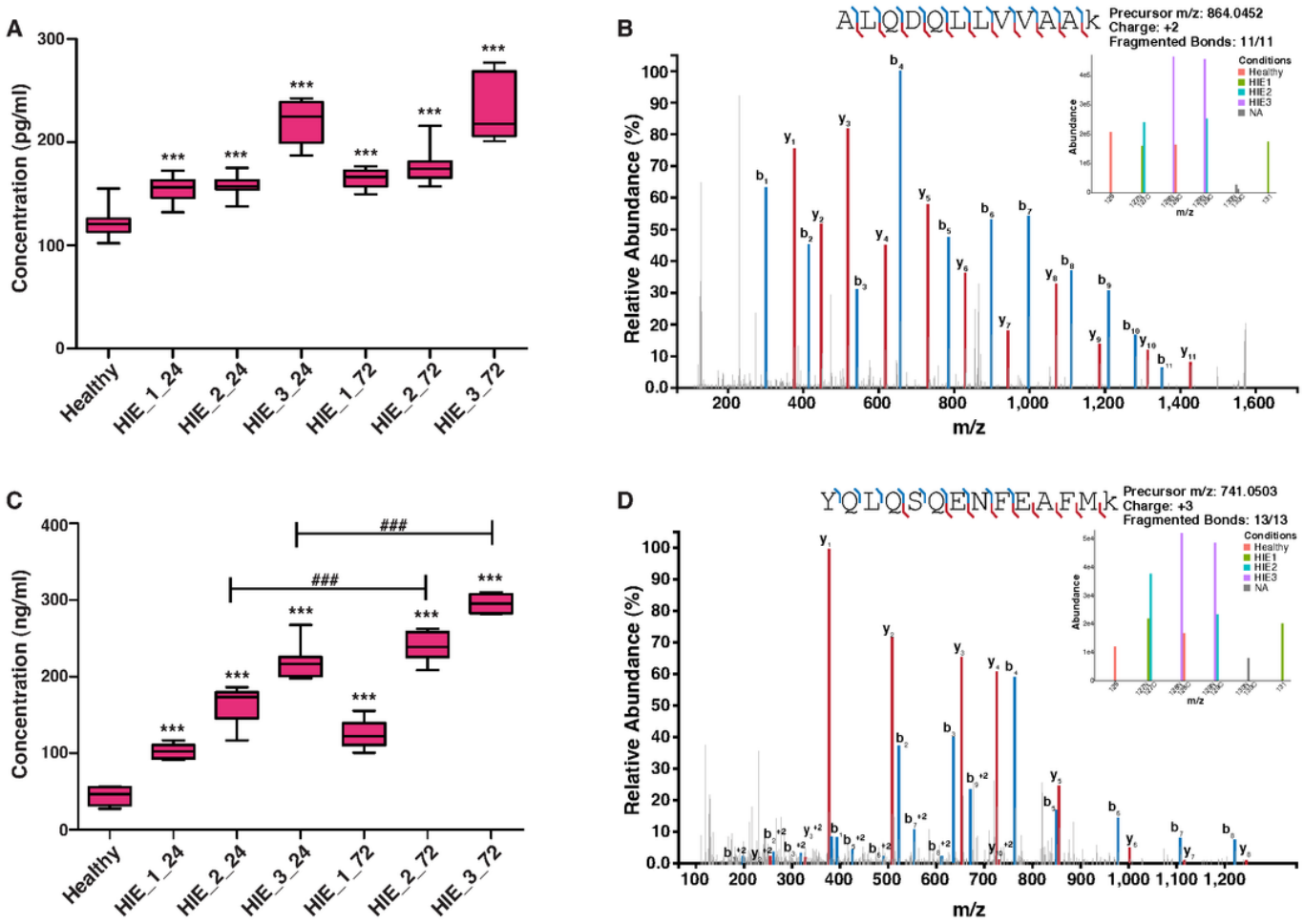

Figure 4

Boxplot (A) and (C) depicts the expression of AGT and FABP1 proteins in asphyxiated neonates at 24 and 72 hours compared to healthy neonates from ELISA. PSM (B) and (D) with respective reporter ion abundances depicts the quality of identification and expression of AGT and FABP1, respectively from proteomics

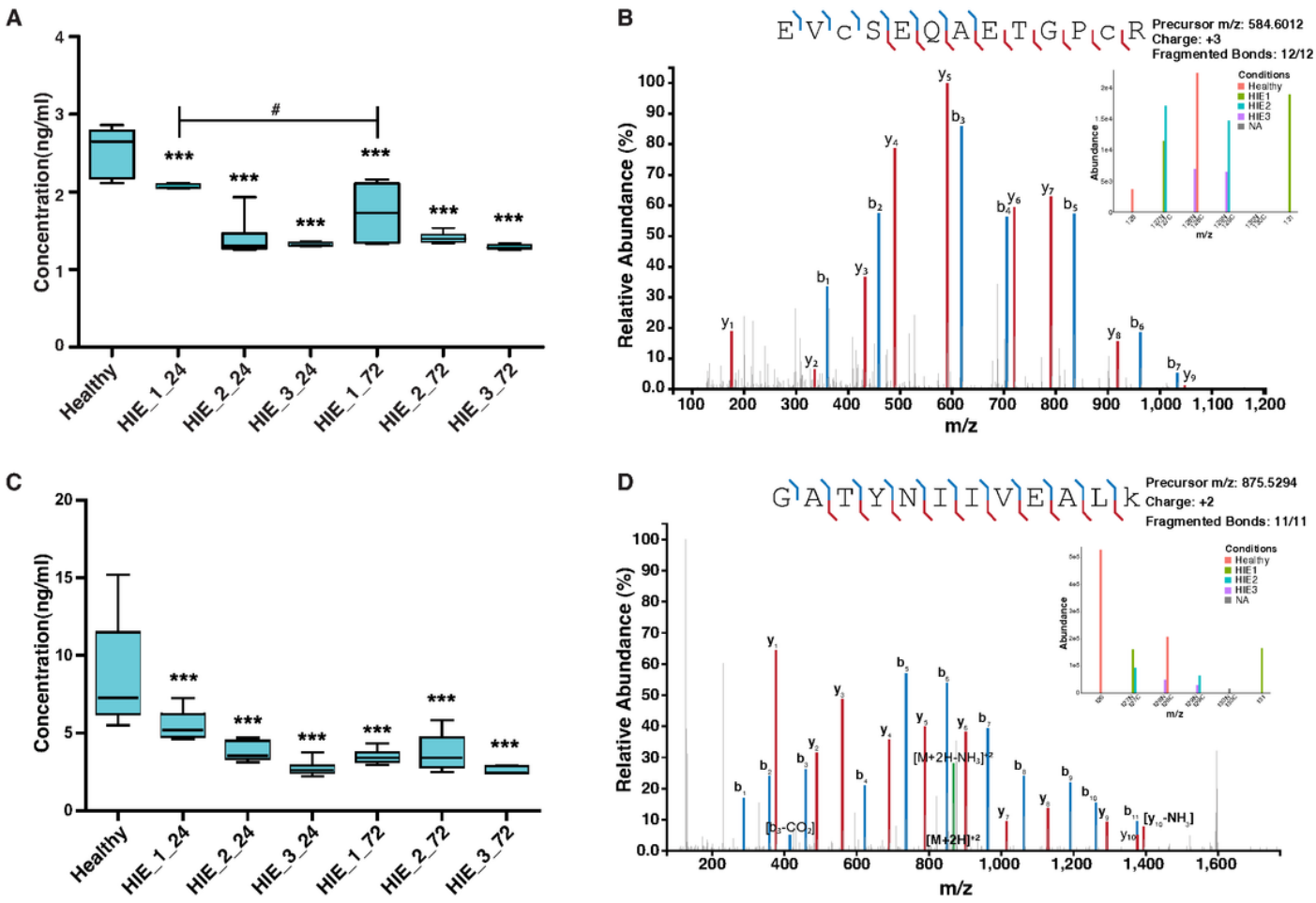

Figure 5

Boxplot (A) and (C) depicts the expression of APP and FN1 proteins in asphyxiated neonates at 24 and 72 hours compared to healthy neonates from ELISA. PSM (B) and (D) with respective reporter ion abundances depicts the quality of identification and expression of APP and FN1, respectively from proteomics

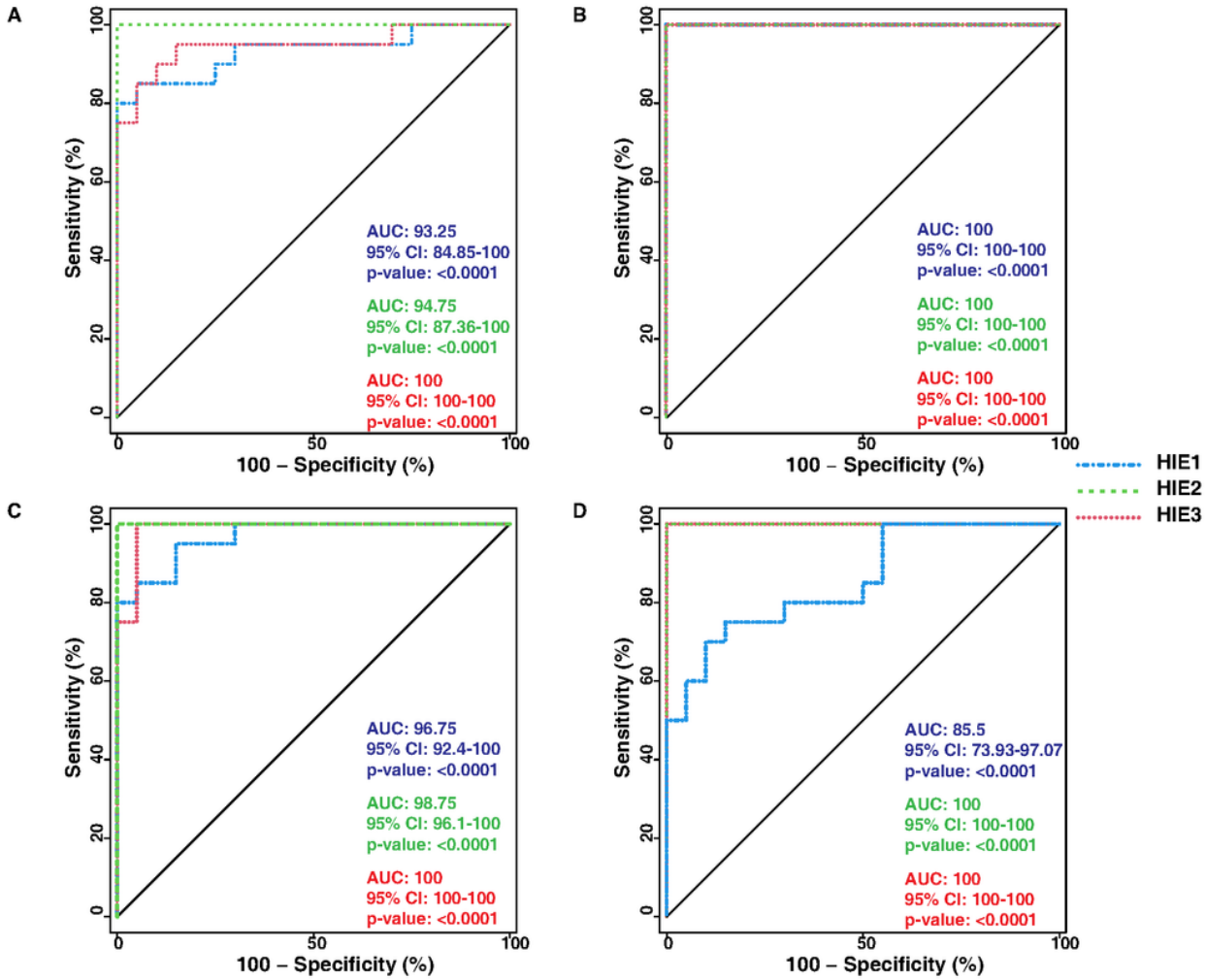

Figure 6

ROC curves for selected panel of proteins (A) AGT (B) FABP1 (C) APP and (D)FN1

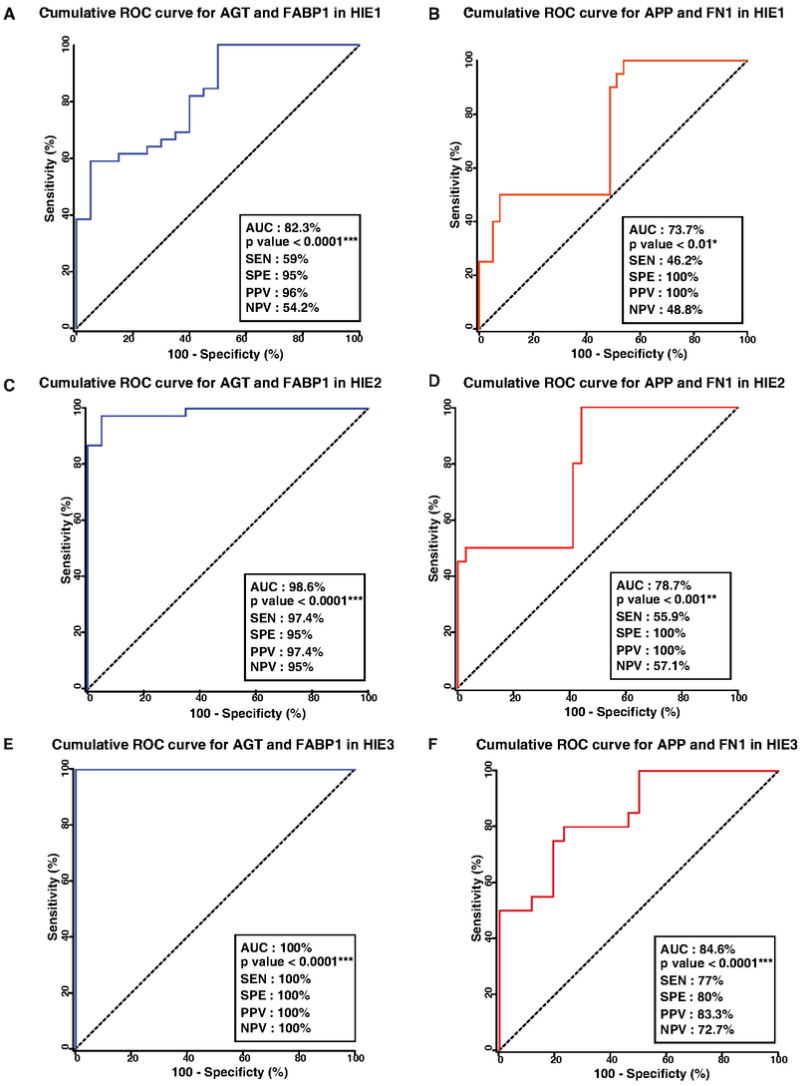

Figure 7

Cumulative ROC curves (A), (C) and (E) depicts the biomarker model for upregulated proteins AGT and FABP1 in HIE1, 2 and 3, respectively. Cumulative ROC curves (B), (D) and (F) depict the biomarker model for downregulated proteins APP and FN1 in HIE1, 2 and 3, respectively

Supplementary Files

This is a list of supplementary files associated with this preprint. Click to download.

- SupplementaryFiles.zip